

Spectral and Raman Analysis of Er^{3+} Doped Zinc Lithium Antimony Sodalime Tellurite Glasses

S.L.Meena

Ceramic Laboratory, Department of physics, Jai Narain Vyas University, Jodhpur 342001(Raj.) India

ABSTRACT

Zinc lithium antimony sodalimetellurite glasses containing Er^{3+} in $(45-x):\text{TeO}_2:10\text{ZnO}:10\text{Li}_2\text{O}:10\text{Sb}_2\text{O}_3:10\text{CaO}:15\text{Na}_2\text{O}:x\text{Er}_2\text{O}_3$. (where $x=1, 1.5, 2$ mol %) have been prepared by melt-quenching method. The amorphous nature of the glasses was confirmed by x-ray diffraction studies. Optical absorption, Excitation, fluorescence and Raman spectra were recorded at room temperature for all glass samples. Judd-Ofelt intensity parameters Ω_λ ($\lambda=2, 4, 6$) are evaluated from the intensities of various absorption bands of optical absorption spectra. Using these intensity parameters various radiative properties like spontaneous emission probability, branching ratio, radiative life time and stimulated emission cross-section of various emission lines have been evaluated.

KEYWORDS: ZLASLT Glasses, Optical Properties, Judd-Ofelt Theory, Raman Analysis.

Date of Submission: 27-10-2021

Date of Acceptance: 10-11-2021

I. INTRODUCTION

Rare-earth ions doped glass-ceramics are important materials for optical fibers, wave guide lasers, sensors and optical amplifiers [1-5]. Oxide glasses are the most stable host matrices for practical applications due to their high chemical durability and thermal stability. The importance of glasses doped with rare earth elements lies in their distinctive emission properties in several electromagnetic spectral regions [6-10]. Tellurite glasses have been extensively investigated due to their transparency in a wide spectral range from the ultraviolet to the infrared, which makes them suitable for the fabrication of optical fibers [11,12]. Tellurite glasses are extremely attractive materials for linear and non-linear application in optics, due to their important aspects such as their low melting temperature, low phonon energy and high refractive index, high dielectric constant, good chemical durability, high thermal stability, non-hygroscopic, with a large transmission window and the possibility to integrate a large amount of rare-earth ions [13-18]. Er^{3+} doped tellurite glasses considerable literature has recently emerged concerning the structure, optical, mechanical, thermal, and electrical properties [19-23].

In this work, the spectroscopic properties of Er^{3+} -doped $(45-x):\text{TeO}_2:10\text{ZnO}:10\text{Li}_2\text{O}:10\text{Sb}_2\text{O}_3:10\text{CaO}:15\text{Na}_2\text{O}:x\text{Er}_2\text{O}_3$ (where $x=1, 1.5, 2$ mol %) glasses were investigated. The optical absorption, Excitation, fluorescence and Raman spectra of Er^{3+} of the glasses were investigated. The intensities of the transitions for the rare earth ions have been estimated successfully using the Judd-Ofelt theory. The laser parameters such as radiative probabilities (A), branching ratio (β), radiative life time (τ_R) and stimulated emission cross section (σ_p) are evaluated using J.O. intensity parameters (Ω_λ , $\lambda=2, 4$ and 6).

II. EXPERIMENTAL TECHNIQUES

Preparation of glasses

The following Er^{3+} doped zinc lithium antimony sodalimetellurite glass samples $(45-x):\text{TeO}_2:10\text{ZnO}:10\text{Li}_2\text{O}:10\text{Sb}_2\text{O}_3:10\text{CaO}:15\text{Na}_2\text{O}:x\text{Er}_2\text{O}_3$ (where $x=1, 1.5, 2$) have been prepared by melt-quenching method. Analytical reagent grade chemical used in the present study consist of $\text{TeO}_2, \text{ZnO}, \text{Li}_2\text{O}, \text{Sb}_2\text{O}_3, \text{CaO}, \text{Na}_2\text{O}$ and Er_2O_3 . All weighed chemicals were powdered by using an Agate pestle mortar and mixed thoroughly before each batch (10g) was melted in alumina crucibles in silicon carbide based an electrical furnace.

Silicon Carbide Muffle furnace was heated to working temperature of 1055°C , for preparation of zinc lithium antimony sodalime tellurite glasses, for two hours to ensure the melt to be free from gases. The melt was stirred several times to ensure homogeneity. For quenching, the melt was quickly poured on the steel plate & was immediately inserted in the muffle furnace for annealing. The steel plate was preheated to 100°C . While pouring; the temperature of crucible was also maintained to prevent crystallization. And annealed at temperature of 350°C for 2h to remove thermal strains and stresses. Every time fine powder of cerium oxide was used for

polishing the samples. The glass samples so prepared were of good optical quality and were transparent. The chemical compositions of the glasses with the name of samples are summarized in Table 1

Table 1 Chemical composition of the glasses

Sample	Glass composition (mol %)
ZLASLT (UD)	45TeO ₂ :10ZnO:10Li ₂ O:10Sb ₂ O ₃ :10CaO:15Na ₂ O
ZLASLT (ER1)	44TeO ₂ :10ZnO:10Li ₂ O:10Sb ₂ O ₃ :10CaO:15Na ₂ O:1 Er ₂ O ₃
ZLASLT (ER 1.5)	43.5TeO ₂ :10ZnO:10Li ₂ O:10Sb ₂ O ₃ :10CaO:15Na ₂ O:1.5 Er ₂ O ₃
ZLASLT (ER2)	43TeO ₂ :10ZnO:10Li ₂ O:10Sb ₂ O ₃ :10CaO:15Na ₂ O: 2 Er ₂ O ₃

ZLASLT (UD)—Represents undoped Zinc Lithium Antimony Sodalime Tellurite glass specimen.

ZLASLT(ER) -Represents Er³⁺ doped Zinc Lithium Antimony Sodalime Tellurite glass specimens.

III. THEORY

3.1 Oscillator Strength

The intensity of spectral lines are expressed in terms of oscillator strengths using the relation [24].

$$f_{\text{expt.}} = 4.318 \times 10^{-9} \int \epsilon(\nu) d\nu \quad (1)$$

where, $\epsilon(\nu)$ is molar absorption coefficient at a given energy ν (cm⁻¹), to be evaluated from Beer–Lambert law. Under Gaussian Approximation, using Beer–Lambert law, the observed oscillator strengths of the absorption bands have been experimentally calculated, using the modified relation [25].

$$P_m = 4.6 \times 10^{-9} \times \frac{1}{cl} \log \frac{I_0}{I} \times \Delta\nu_{1/2} \quad (2)$$

where c is the molar concentration of the absorbing ion per unit volume, l is the optical path length, $\log I_0/I$ is absorbivity or optical density and $\Delta\nu_{1/2}$ is half band width.

3.2. Judd-Ofelt Intensity Parameters

According to Judd [26] and Ofelt [27] theory, independently derived expression for the oscillator strength of the induced forced electric dipole transitions between an initial J manifold $|4f^N(S, L) J\rangle$ level and the terminal J' manifold $|4f^N(S', L') J'\rangle$ is given by:

$$\frac{8\pi^2 mc \nu}{3h(2J+1)n} \frac{1}{n} \left[\frac{(n^2+2)^2}{9} \right] \times S(J, J') \quad \text{where, the} \quad (3)$$

line strength $S(J, J')$ is given by the equation

$$S(J, J') = e^2 \sum_{\lambda} \Omega_{\lambda} \langle 4f^N(S, L) J \| U^{(\lambda)} \| 4f^N(S', L') J' \rangle^2 \quad (4)$$

$\lambda = 2, 4, 6$

In the above equation m is the mass of an electron, c is the velocity of light, ν is the wave number of the transition, h is Planck's constant, n is the refractive index, J and J' are the total angular momentum of the initial and final level respectively, Ω_{λ} ($\lambda = 2, 4$ and 6) are known as Judd-Ofelt intensity parameters.

3.3. Radiative Properties

The Ω_{λ} parameters obtained using the absorption spectral results have been used to predict radiative properties such as spontaneous emission probability (A) and radiative life time (τ_R), and laser parameters like fluorescence branching ratio (β_R) and stimulated emission cross section (σ_p).

The spontaneous emission probability from initial manifold $|4f^N(S', L') J'\rangle$ to a final manifold $|4f^N(S, L) J\rangle$ is given by:

$$A[(S', L') J'; (S, L) J] = \frac{64\pi^2 \nu^3}{3h(2J'+1)} \left[\frac{n(n^2+2)^2}{9} \right] \times S(J', \bar{J}) \quad (5)$$

$$\text{Where, } S(J', J) = e^2 [\Omega_2 \| U^{(2)} \|^2 + \Omega_4 \| U^{(4)} \|^2 + \Omega_6 \| U^{(6)} \|^2]$$

The fluorescence branching ratio for the transitions originating from a specific initial manifold $|4f^N(S', L') J'\rangle$ to a final manifold $|4f^N(S, L) J\rangle$ is given by

$$\beta[(S', L') J'; (S, L) J] = \frac{A[(S'L)]}{\sum A[(S'L)J'(SL)]} \quad (6)$$

S, L, J

where, the sum is over all terminal manifolds.

The radiative life time is given by

$$\tau_{rad} = \sum_{S, L, J} A[(S', L') J'; (S, L) J] = A_{Total}^{-1} \quad (7)$$

S L J

where, the sum is over all possible terminal manifolds. The stimulated emission cross-section for a transition from an initial manifold $|4f^N(S', L') J' \rangle$ to a final manifold $|4f^N(S, L) J \rangle$ is expressed as

$$\sigma_p(\lambda_p) = \left[\frac{\lambda_p^4}{8\pi c n^2 \Delta\lambda_{eff}} \right] \times A[(S', L') J'; (\bar{S}, \bar{L}) \bar{J}] \quad (8)$$

where, λ_p the peak fluorescence wavelength of the emission band and $\Delta\lambda_{eff}$ is the effective fluorescence line width.

3.4 Nephelauxetic Ratio (β') and Bonding Parameter ($b^{1/2}$)

The nature of the R-O bond is known by the Nephelauxetic Ratio (β') and Bonding Parameters ($b^{1/2}$), which are computed by using following formulae [28, 29]. The Nephelauxetic Ratio is given by

$$\beta' = \frac{\nu_g}{\nu_a} \quad (9)$$

where, ν_a and ν_g refer to the energies of the corresponding transition in the glass and free ion, respectively. The value of bonding parameter ($b^{1/2}$) is given by

$$b^{1/2} = \left[\frac{1 - \beta'}{2} \right]^{1/2} \quad (10)$$

IV. RESULT AND DISCUSSION

4.1. XRD Measurement

Figure 1 presents the XRD pattern of the samples containing show no sharp Bragg's peak, but only a broad diffuse hump around low angle region. This is the clear indication of amorphous nature with in the resolution limit of XRD instrument.

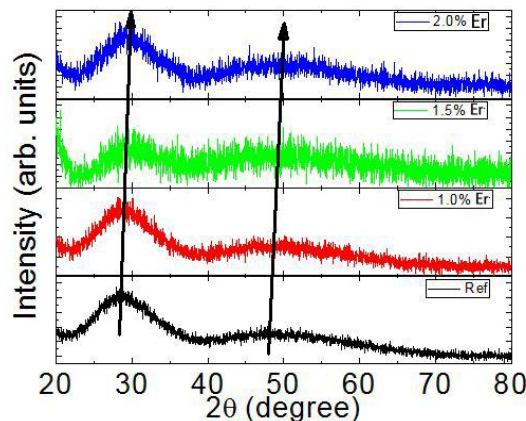


Fig.1: X-ray diffraction pattern of ZLASLT(ER) glasses.

4.2 Raman spectra

The Raman spectrum of Zinc Lithium Antimony Sodalime Tellurite (ZLASLT) glass specimens is recorded and is shown in Fig. 2. The Raman band at 120 cm^{-1} corresponds to bending mode of Te-O-Te, which is formed by sharing vertices of TeO_4 tetrahedra, TeO_{3+1} polyhedra and TeO_3 trigonal groups; stretching over long distance in the glass network. The Raman band at 450 cm^{-1} is usually ascribed to bending vibrations of Te-O-Te linkages. The Raman bands around 675 and 750 cm^{-1} are assigned to stretching vibrations in TeO_4 and TeO_3 groups, respectively. The increase in intensity observed for the 750 cm^{-1} band with erbium concentration is consistent with the destruction of TeO_4 groups.

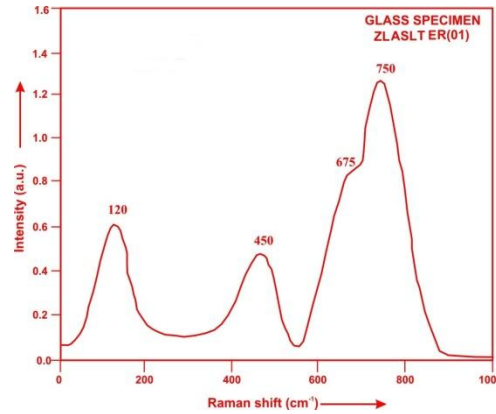


Fig. (2) Raman spectrum of ZLASLTER (01) glass.

4.2. Absorption spectra

The absorption spectra of ZLASLTER(01) glass, consists of absorption bands corresponding to the absorptions from the ground state $^4I_{15/2}$ of Er^{3+} ions. Ten absorption bands have been observed from the ground state $^4I_{15/2}$ to excited states $^4I_{11/2}$, $^4I_{9/2}$, $^4F_{9/2}$, $^4S_{3/2}$, $^2H_{11/2}$, $^4F_{7/2}$, $^4F_{5/2}$, $^4F_{3/2}$, $^2H_{9/2}$ and $^4G_{11/2}$ for Er^{3+} doped ZLASLTER (01) glass.

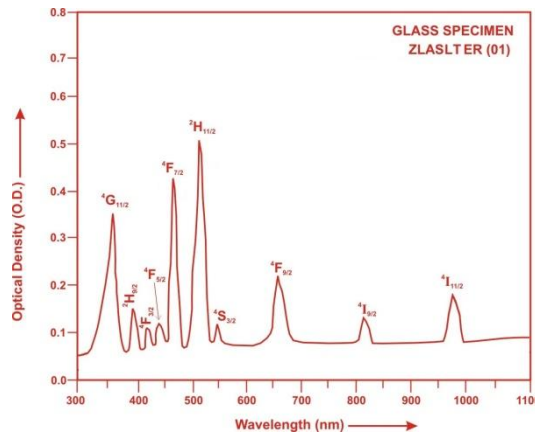


Fig.2: Absorption spectra of ZLASLTER(01) glass.

The experimental and calculated oscillator strengths for Er^{3+} ions in zinc lithium antimony sodalime tellurite glasses are given in Table 2

Table 2. Measured and calculated oscillator strength ($P^m \times 10^{+6}$) of Er^{3+} ions in ZLASLT glasses.

Energy level	Glass ZLASLT (ER01)		Glass ZLASLT (ER1.5)		Glass ZLASLT (ER02)	
$^4I_{15/2}$	$P_{exp.}$	$P_{cal.}$	$P_{exp.}$	$P_{cal.}$	$P_{exp.}$	$P_{cal.}$
$^4I_{11/2}$	0.88	0.66	0.85	0.66	0.82	0.65
$^4I_{9/2}$	0.44	0.14	0.41	0.13	0.39	0.13
$^4F_{9/2}$	2.45	1.42	2.42	1.41	2.38	1.40
$^4S_{3/2}$	0.38	0.60	0.36	0.59	0.33	0.59
$^2H_{11/2}$	6.58	2.40	6.55	2.41	6.51	2.41
$^4F_{7/2}$	5.30	2.08	5.25	2.07	5.20	2.05
$^4F_{5/2}$	0.67	0.76	0.64	0.75	0.61	0.74
$^4F_{3/2}$	0.38	0.47	0.35	0.46	0.32	0.46
$^2H_{9/2}$	1.68	0.89	1.65	0.98	1.62	0.88
$^4G_{11/2}$	4.85	6.78	4.83	6.78	4.79	6.77
R.m.s.deviation	1.8283		1.8129		1.7989	

The various energy interaction parameters like Slater-Condon parameters F_k ($k=2, 4, 6$), Lande' parameter (ξ_{4f}) and Racah parameters E^k ($k=1, 2, 3$) have been computed using partial regression. Computed values of Slater-Condon, Lande', Racah, nephelauxetic ratio and bonding parameter for Er^{3+} doped ZLASLT glass specimens are given in Table 3.

Table 3. Computed values of Slater-Condon, Lande', Racah, nephelauxetic ratio and bonding parameter for Er³⁺ doped ZLASLT glass specimens.

Parameter	Free ion	ZLASLTER01	ZLASLTER1.5	ZLASLTER02
F ₂ (cm ⁻¹)	441.680	433.951	433.944	433.965
F ₄ (cm ⁻¹)	68.327	67.045	67.043	67.044
F ₆ (cm ⁻¹)	7.490	7.045	7.043	7.046
ξ _{4f} (cm ⁻¹)	2369.400	2414.646	2414.708	2414.632
E ¹ (cm ⁻¹)	6855.300	6663.138	6662.629	6663.316
E ² (cm ⁻¹)	32.126	31.348	31.346	31.350
E ³ (cm ⁻¹)	645.570	643.641	643.681	643.647
F ₂ /F ₂	0.15470	0.154499	0.1544968	0.1544917
F ₆ /F ₂	0.01696	0.01623455	0.01623020	0.01623633
E ¹ /E ³	10.61899	10.352258	10.350824	10.352439
E ² /E ³	0.049764	0.048704	0.048698	0.048707
β'		0.99577279	.99567274	.99579898
b ^{1/2}		0.045973986	0.046514838	0.045831333

Judd-Ofelt intensity parameters Ω_λ ($\lambda = 2, 4$ and 6) were calculated by using the fitting approximation of the experimental oscillator strengths to the calculated oscillator strengths with respect to their electric dipole contributions. In the present case the three Ω_λ parameters follow the trend $\Omega_4 < \Omega_2 < \Omega_6$.

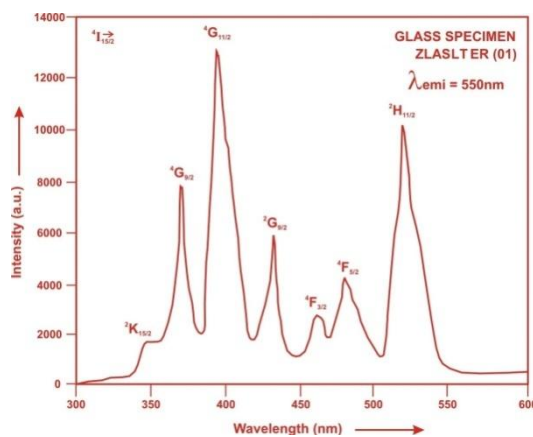
The values of Judd-Ofelt intensity parameters are given in Table 4.

Table 4. Judd-Ofelt intensity parameters for Er³⁺ doped ZLASLT glass specimens.

Glass Specimen	Ω_2 (pm ²)	Ω_4 (pm ²)	Ω_6 (pm ²)	Ω_4/Ω_6
ZLASLT (ER01)	0.8612	0.2944	0.9350	0.3149
ZLASLT (ER1.5)	0.8676	0.2921	0.9300	0.3141
ZLASLT (ER02)	0.8704	0.2890	0.9202	0.3141

4.4 Excitation Spectrum

The Excitation spectra of Er³⁺ doped ZLASLT glass specimens have been presented in Figure 4 in terms of Excitation Intensity versus wavelength. The excitation spectrum was recorded in the spectral region 300–600 nm fluorescence at 550nm having different excitation band centered at 350, 365, 381, 425, 450, 470 and 515 nm are attributed to the ²K_{15/2}, ⁴G_{9/2}, ⁴G_{11/2}, ²G_{9/2}, ⁴F_{3/2}, ⁴F_{5/2} and ²H_{11/2} transitions, respectively. The highest absorption level is ⁴G_{11/2} and is at 381nm. So this is to be chosen for excitation wavelength.

**Fig.4:** Excitation Spectrum of ZLASLTER (01) glass.

4.3. Fluorescence Spectrum

The fluorescence spectrum of Er³⁺ doped in zinc lithium antimony sodalime tellurite glass is shown in Figure 3. There are seven broad bands (⁴F_{7/2}→⁴I_{15/2}), (²H_{11/2}→⁴I_{15/2}), (⁴S_{3/2}→⁴I_{15/2}), (⁴F_{9/2}→⁴I_{15/2}), (⁴I_{11/2}→⁴I_{15/2}), (⁴I_{13/2}→⁴I_{15/2}) and (⁴I_{11/2}→⁴I_{13/2}) respectively for glass specimens.

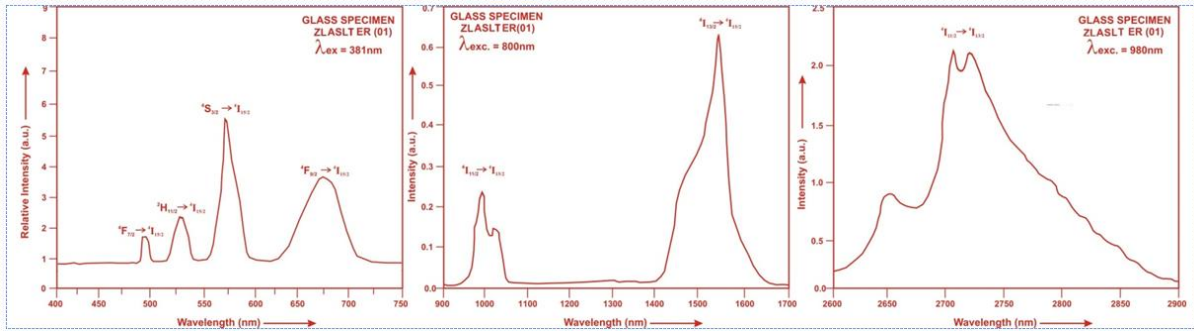


Fig.3: Fluorescence spectrum of ZLASLTER (01) glass.

Table 5. Emission peak wave lengths (λ_p), radiative transition probability (A_{rad}), branching ratio (β_R), stimulated emission crosssection (σ_p), and radiative life time (τ) for various transitions in Er³⁺ doped ZLASLT glasses.

Transition	ZLASLTER 01					ZLASLTER 1.5					ZLASLTER 02			
	λ_{max} (nm)	$A_{rad}(s^{-1})$	β	$\sigma_p (10^{-20} cm^2)$	$\tau_R (\mu s)$	$A_{rad}(s^{-1})$	β	$\sigma_p (10^{-20} cm^2)$	$\tau_R (\mu s)$	$A_{rad}(s^{-1})$	β	$\sigma_p (10^{-20} cm^2)$	$\tau_R (10^{-20} cm^2)$	
$^4F_{7/2} \rightarrow ^4I_{15/2}$	485	1956.35	0.4047	0.5282		1949.45	0.4037	0.5207		1932.76	0.4025	0.5060		
$^2H_{11/2} \rightarrow ^4I_{15/2}$	530	1234.31	0.2553	0.3909		1241.48	0.2571	0.3896		1244.33	0.2592	0.3837		
$^4S_{3/2} \rightarrow ^4I_{15/2}$	550	867.76	0.1795	0.2617		864.85	0.1791	0.2588		856.99	0.1785	0.2514		
$^4F_{9/2} \rightarrow ^4I_{15/2}$	657	581.20	0.1202	0.3089	206.84	579.14	0.1199	0.3038	207.07	573.91	0.1195	0.2959	208.29	
$^4I_{13/2} \rightarrow ^4I_{15/2}$	990	100.43	0.0208	0.3559		100.17	0.0207	0.3492		99.43	0.02071	0.3410		
$^4I_{13/2} \rightarrow ^4I_{15/2}$	1538	80.99	0.0168	1.2059		80.74	0.01672	1.1874		80.06	0.01672	1.1573		
$^4I_{11/2} \rightarrow ^4I_{15/2}$	2711	13.59	0.0028	0.7802		13.55	0.0028	0.7718		13.44	0.0028	0.7580		

V. CONCLUSION

In the present study, the glass samples of composition (45-x)TeO₂:10ZnO:10Li₂O:10Sb₂O₃:10CaO:15Na₂O:xEr₂O₃ (where x=1, 1.5, 2 mol %) have been prepared by melt-quenching method. The value of stimulated emission cross-section (σ_p) is found to be maximum for the transition ($^4I_{13/2} \rightarrow ^4I_{15/2}$) for glass ZLASLT (ER 01), suggesting that glass ZLASLT (ER 01) is better compared to the other two glass systems ZLASLT(ER1.5) and ZLASLT (ER02). A Raman band, associated with the Te–O–Te vibration mode has been observed near 450 cm⁻¹. It was found that this band shows a significant decrease in intensity as the Er³⁺ ion concentration increases, indicating a structural disruption in the glass network due to the erbium increasing.

REFERENCES

- [1]. Deopa, N., Kumar, B., Sahu, M. K., Rani, P. R. and Rao, A. S. (2019). Effect of Sm³⁺ ions concentration on borosilicate glasses for reddish orange luminescent device applications. *J. Non-Cryst. Solids*, 513, 152-158.
- [2]. Meza-Rocha, A. N., Bordignon, S., Speghini, A., Lozada-Morales, R. and Caldino, U. (2018). Zinc phosphate glasses activated with Dy³⁺/Eu³⁺/Sm³⁺ and Tb³⁺/Eu³⁺/Sm³⁺ for reddish-orange and yellowish white phosphor applications. *J. Lumin.* 203, 74-82.
- [3]. Rao, V. R. and Jayasankar, C. K. (2019). Spectroscopic investigation on multi-channel visible and NIR emission of Sm³⁺ doped alkali-alkaline earth fluoro phosphate glasses. *Opt. Mater.* 91, 7-16.
- [4]. Largot, H., Aiadi, K. E., Ferid, M., Haraiech, S., Bouzidi, C., Charnay, C. and Horchani-Naifer, K. (2019). Spectroscopic investigations of Sm³⁺ doped phosphate glasses: Judd-Ofelt analysis. *Phys. B Condens. Matter*, 552, 184-189.
- [5]. Wu, T., Cheng, Y., Zhong, H., Peng, H. and Hu, J. (2018). Thermal Stability and Spectral Properties of Tm³⁺, Yb³⁺ doped Tellurite Glasses. *Glass Phys. Chem.*, 44, 163-169.
- [6]. Çelikkilek-Ersundu, M. and Ersundu, A. E. (2016). Structure and crystallization kinetics of lithium tellurite glasses. *J. Non-Cryst. Solids*, 453, 150-157.
- [7]. Mogoš-Milanković, A., Pavić, L., Reis, S. T., Day, D. E. and Ivanda, M. (2010). Structural and electrical properties of Li₂O–ZnO–P₂O₅ glasses. *J. Non-Cryst. Solids*, 356, 715-719.
- [8]. Balda, R., García-Revilla, S., Fernández, J., Seznec, V., Nazabal, V., Zhang, X. H., Adam, J. L., Allix, M. and Matzen, G. (2009). Upconversion luminescence of transparent Er³⁺-doped chalcogenide glass-ceramics. *Opt. Mater.* 31, 760-764.
- [9]. Assadi, A. A., Damak, K. and Lachheb, R. (2015). Spectroscopic and luminescence characteristics of erbium doped TNZL glass for laser materials. *Journal of Alloys and Compounds*, 620, 129-136.
- [10]. Situmorang, R., Marbun, A., Hakim, A., Panggabean, D. D., Rajagukguk, J. and Kaewkhao, J. (2018). Preparation and characterization of Nd³⁺ doped P₂O₅-Bi₂O₃-Na₂O-Gd₂O₃ glasses system for laser medium application. *J. Phys.: Conf. Ser.* 1120, 1-9.

- [11]. Kesavulu, C. Kim, H. J., Lee, S. W., Kaewkhao, J., Wantana, N., Kaewnuam, E., Kothand, S. and Kaewjaeng, S. (2017). Spectroscopic investigations of Nd³⁺ doped gadolinium calcium silica borate glasses for the NIR emission at 1059nm, *J. Alloys. Compd.*, 695, 590-590.
- [12]. Lalla, E. A., León-Luis, S. F., Monteseuro, V., Pérez-Rodríguez, C., Cáceres, J. M., Lavín, V. and Rodríguez-Mendoza, U. R. (2015). Optical temperature sensor based on the Nd³⁺ infrared thermalized emissions in a fluorotellurite glass, *J. Lumin.* 166, 209–214.
- [13]. Kaky, Kawa M., Sayyed, M. I., Laariedh, F., Abdalsalam, Alyaa H., Tekin, H. O. and Baki, S. O. (2019). Structural, optical and radiation shielding properties of zinc boro-tellurite alumina glasses. *Applied Physics A* 125, no. 1, 1-12.
- [14]. Sun, Hong-tao, Lei Wen, Zhong-chao Duan, Li-li Hu, Jun-jie Zhang and Zhong-hong Jiang. (2006). Intense frequency upconversion fluorescence emission of Er³⁺/Yb³⁺-codoped oxochloride germanate glass. *Journal of Alloys and Compounds* 414, no. 1-2, 142-145.
- [15]. Wang, J. S., Vogel, E. M., Snitzer, E. (1994). Tellurite glass: a new candidate for fiber devices, *Opt. Mater.* 3, 187-203.
- [16]. Jha, A., Richards, B., Jose, G., Teddy-Fernandez, T., Joshi, P., Jiang, X. and Lousteau, J. (2012). Rare-earth ion doped TeO₂ and GeO₂ glasses as laser materials, *Prog. Mater. Sci.* 57, 1426-1491.
- [17]. Sharudin Omar, Baki, Tan, L. S., Kan, C. S., Kamari, H. M., Noor, A. S. M. and Mahdi, M. A. (2014). Spectroscopic Studies of Er³⁺-Yb³⁺ Co-doped Multicomposition Tellurite Oxide Glass. *Sains Malaysiana* 43, no. 6, 843-850.
- [18]. Jha, A., Richards, B. D. O., Jose, G., Fernandez, T. T., Hill, C. J., Lousteau, J. and Joshi, P. (2012). Review on structural, thermal, optical and spectroscopic properties of tellurium oxide based glasses for fiber optic and waveguide applications, *Int. Mater. Rev.* 57, 357-382.
- [19]. León-Luis, S. F., Rodríguez-Mendoza, U. R., Martín, I. R., Lalla, E., and Lavín, V. (2013). Effects of Er³⁺ concentration on thermal sensitivity in optical temperature fluorotellurite glass sensors, *Sens. Actuators B Chem.* 176, 1167– 1175.
- [20]. Vijaya, N., Babu, P., Venkatramu, V., Jayasankar, C. K., León-Luis, S. F., Rodríguez-Mendoza, U. R., Martín, I. R. and Lavín, V. (2013). Optical characterization of Er³⁺-doped zinc fluorophosphate glasses for optical temperature sensors, *Sens. Actuators B Chem.* 186, 156–164.
- [21]. Tian, Y., Huang, P., Wang, L., Shi, Q. and Cui, C. E. (2016). Effect of Yb³⁺ concentration on upconversion luminescence and temperature sensing behavior in Yb³⁺/Er³⁺ co-doped YNbO₄ nanoparticles prepared via molten salt route, *Chem. Eng. J.* 297, 26–34.
- [22]. Prabhu, N. S., Hegde, V., Sayyed, M. I., Agar, O. and Kamath, S. D. (2019). Investigations on structural and radiation shielding properties of Er³⁺ doped zinc bismuth borate glasses, *Materials chemistry and physics*, 230, 267-276.
- [23]. Othman, H. A., Alqahtani, M. M., Reben, M. and Yousef, E. S. (2020). Raman gain and structural of tellurite-phosphate glasses with different modifiers doping with Er₂O₃. *Chalcogenide Letters*, 17, 207 – 215.
- [24]. Gorller-Walrand, C. and Binnemans, K. (1988). Spectral Intensities of f-f Transition. In: Gshneider Jr., K. A. and Eyring, L., Eds., *Handbook on the Physics and Chemistry of Rare Earths*, Vol. 25, Chap. 167, North-Holland, Amst., 101.
- [25]. Sharma, Y. K., Surana, S. S. L. and Singh, R. K. (2009). Spectroscopic Investigations and Luminescence Spectra of Sm³⁺ Doped Soda Lime Silicate Glasses. *Journal of Rare Earths*, 27, 773.
- [26]. Judd, B. R. (1962). Optical Absorption Intensities of Rare Earth Ions. *Physical Review*, 127, 750.
- [27]. Ofelt, G. S. (1962). Intensities of Crystal Spectra of Rare Earth Ions. *The Journal of Chemical Physics*, 37, 511.
- [28]. Sinha, S. P. (1983). Systematics and properties of lanthanides, Reidel, Dordrecht.
- [29]. Krupke, W. F. (1974). *IEEE J. Quantum Electron* QE, 10, 450.

S.L.Meena, "Spectral and Raman Analysis of Er³⁺ Doped Zinc Lithium Antimony Sodalime Tellurite Glasses." *International Journal of Engineering Science Invention (IJESI)*, Vol. 10(11), 2021, PP 09-15. Journal DOI- 10.35629/6734